

# OPTIMIZATION OF OTR SCREEN SURFACE MATERIALS AND OTR SCREEN GEOMETRY AT CTF3

C.P. Welsch, E. Bravin and T. Lefèvre

CERN, Geneva, Switzerland

Received: September 03, 2008

**Abstract.** Optical transition radiation (OTR) has proven to be a flexible and effective tool for measuring a wide range of beam parameters and is of particular importance for online measurements of the transverse and longitudinal beam profile. It is today an established and widely used diagnostic method providing real-time measurements that scale linear with the beam charge. Measurements in the CLIC Test Facility (CTF3) showed that different factors were limiting the overall performance of the installed profile monitors. In this paper, these factors are identified and possible countermeasures discussed. In particular, the influence of the surface material of the OTR screen itself as well as its shape on the emitted light is addressed.

## 1. INTRODUCTION

Optical transition radiation (OTR) [1-3] provides a signal in the visible range that increases linear with the bunch charge and furthermore offers a spatial resolution that may range down to values as small as some  $\mu\text{m}$  [4].

If a charge  $q$  hits a boundary surface with an oblique incidence, the emitted electric field has two components: One in the plane of observation and the other one perpendicular to it. The total emitted intensity  $W$  of a beam with a given relativistic  $\gamma$  therefore has to be calculated as the sum of these two components [2]

$$\frac{d^2 W}{d\Omega d\omega} = \frac{d^2 W_{\parallel}}{d\Omega d\omega} + \frac{d^2 W_{\perp}}{d\Omega d\omega} \approx \frac{q^2}{\pi^2 c} \frac{\theta^2}{(\gamma^{-2} + \theta^2)^2} \quad (1)$$

The number of OTR photons  $N_{OTR}$  that are created within a specific wavelength interval between  $\lambda_a$  and  $\lambda_b$  at a beam energy  $\gamma$  is given by [1]

$$N_{OTR} = \frac{2\alpha}{\pi} \ln\left(\frac{\lambda_b}{\lambda_a}\right) [\ln(2\gamma) - 1/2], \quad (2)$$

where the fine structure constant  $\alpha = e^2 / (\hbar c) \approx 1/137$  was used.

The relative OTR emission intensity as a function of the emission angle depends on various parameters, among which is the energy of the incident electron beam. By differentiating Eq. (1), the maximum of the OTR light distribution is found at an emission angle of  $\theta = 1/\gamma$ , i.e. the emitted light cone gets narrower with increasing beam energy. In the energy range covered at CTF3 [5,6], this opening angle varies between  $2.3^\circ$  (25 MeV) and  $0.4^\circ$  (160 MeV).

As an example, the OTR distribution of a 150 MeV electron beam passing through a thin aluminium foil is shown in Fig. 1.

## 2. MEASUREMENTS AT CTF3

In CTF3, OTR screens are used for machine optimization, emittance measurements, and studies of beam dispersion in several spectrometer lines. With

Corresponding author: Dr. Carsten P. Welsch, e-mail: Carsten.Welsch@cern.ch

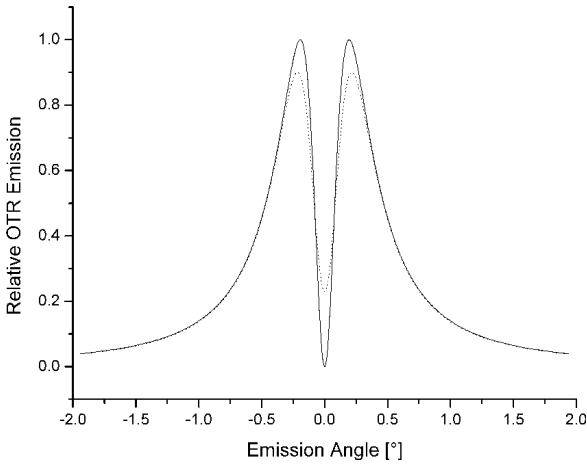


**Fig. 1.** Angular distribution of transition radiation as a function of the emission angle  $\theta$  for a 150 MeV electron beam with (—) and without (---) a beam divergence of 1 mrad.

the aim to get a better understanding of the characteristics and, in particular, the present limitations of the optical systems used in CTF3 and to find possible improvements, systematic measurements at 68 MeV, 95 MeV, and 125 MeV were carried out and associated simulations were done, testing different OTR screen materials and shapes [7].

In the spectrometer lines, relatively large OTR screens with an effective screen area of 100 mm x 40 mm, where an OTR foil is clamped in between the two parts of a rectangular support, are installed. During a typical measurement, the electron beam is swept over a distance from -30 mm to +30 mm relative to the screen centre and the intensity across the screen is recorded. A typical result of such a scan is shown in the following Fig. 2. where an electron beam at energy  $E=73$  MeV was used.

Two things shall be pointed out: first, the relative illumination decreases rapidly as the distance from the screen centre increases - an effect that will be discussed in detail in the following section. Second, a second peak in the centre occurs when moving towards the screen edges.

When the electrons are bent in the spectrometer line, they emit synchrotron radiation (SR), which is reflected by the OTR screen and may degrade the performances of the monitors. Since the photons are not generated at the same longitudinal position, the SR light increases the noise level of the measurement and distorts the beam shape. To understand this effect also quantitatively, SR

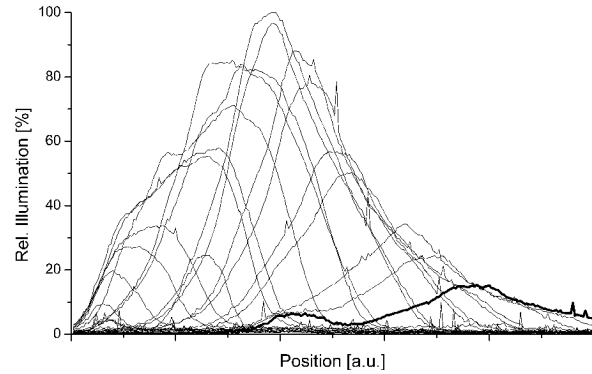


**Fig. 2.** Measured relative illumination across the OTR screen at a beam energy of  $E=73$  MeV.

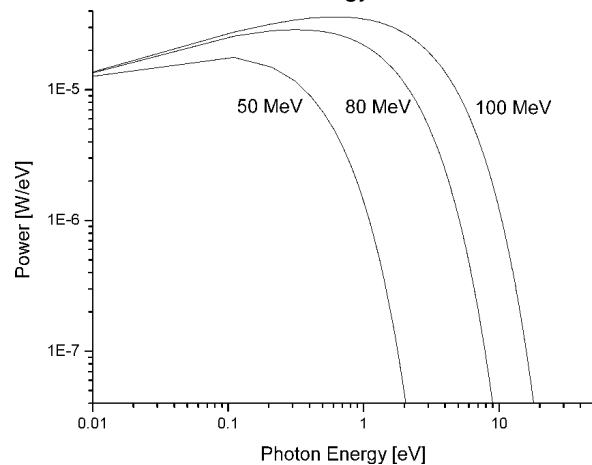


**Fig. 3.** Synchrotron light spectrum in the spectrometer line. Calculations assume that a 5.4 A current beam is bent by  $23^\circ$  and that the distance between the centre of the magnet and the screen is 1 m.

**Table 1.** Number of emitted photons/electron in case of SR and OTR at different energies.

Beam Energy [MeV]	# Photons/ Electron (SR)	# Photons/ Electron (OTR)
50	$1.5 \cdot 10^{-9}$	$7.7 \cdot 10^{-3}$
80	$5 \cdot 10^{-4}$	$8.6 \cdot 10^{-3}$
100	$4 \cdot 10^{-3}$	$9 \cdot 10^{-3}$

spectrums have been calculated using the program XOP [8] for our beam parameters and the results are presented in Fig. 3. In order to get the number of photons produced by SR in the dipole, these spectra are integrated between 2 and 3eV and compared to OTR yield calculations resulting from

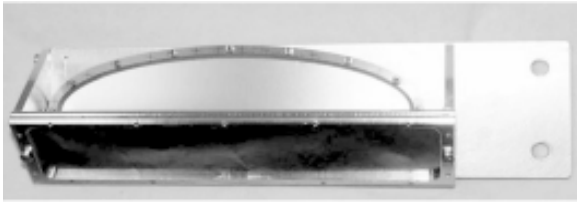


**Fig. 4.** Photograph of the oval OTR screen used in the CTF3 spectrometer lines with the mounted synchrotron light shielding.

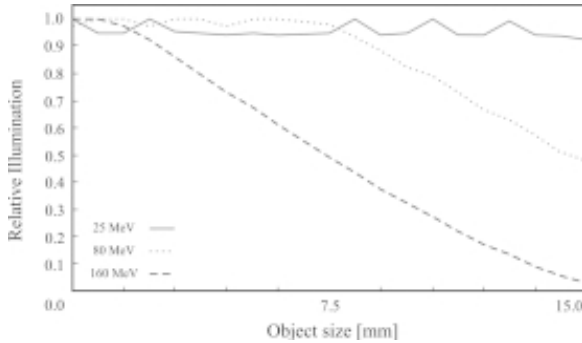


**Fig. 5.** Relative illumination of the CCD chip at different beam energies.

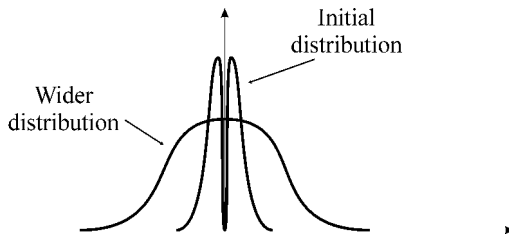


**Fig. 6.** Illustration of the artificial widening of the OTR light distribution.

(2). The results are summarized in Table 1. For electron energies higher than 80 MeV, the amount of SR produced in the bending magnet is comparable to the intensity of the OTR light and thus strongly degrades the accuracy of each measurement. In order to efficiently stop the SR photons a 50 mm carbon foil was implemented a few cm in front of the OTR screen as shown in Fig. 4. This shielding is today an integral part of all spectrometer screens and allows efficiently suppressing the SR while maintaining the high resulting for the measurements.

As pointed out before, measurements at higher energies showed a rapid decrease in relative illumination of the screen towards its edges. Calculations with the ZEMAX code [9] revealed that this

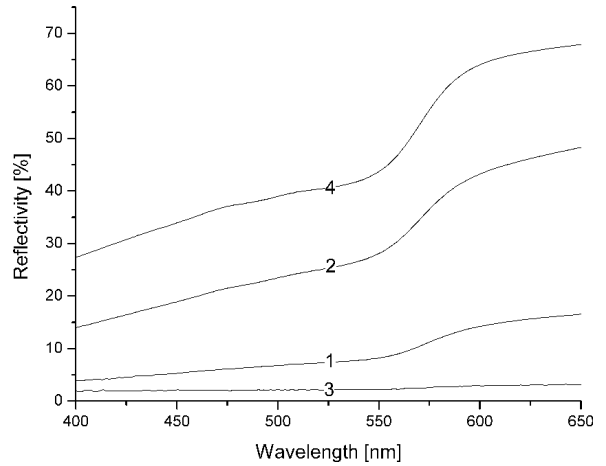


**Fig. 7.** Reflectivity of a copper plate after different treatments.

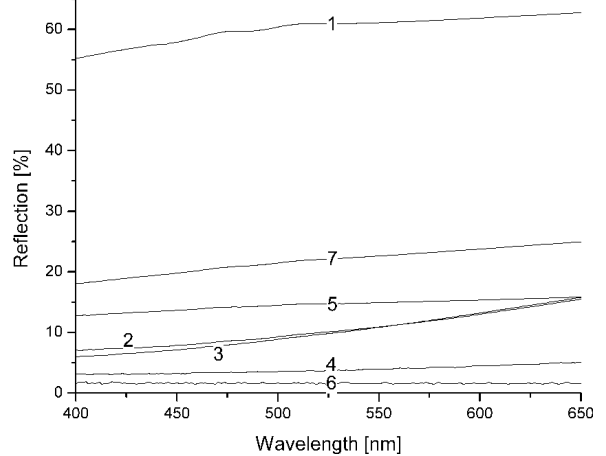


**Fig. 8.** Reflectivity of a stainless steel plate after different treatments.

effect is caused by the narrower intensity distribution of the emitted radiation at higher energies and the subsequent vignetting caused by the imaging system. The results of these simulations are summarized in Fig. 5 and comply with the measured data.

### 3. SURFACE TREATMENTS

A possible approach to improve on the existing situation is to artificially recreate the low-energy light distribution by using a diffusive OTR screen. If one could control the opening angle of the emitted radiation which results from the sum of the OTR and the diffusive characteristics of the screen surface itself, this could open up a way for a homogenous light distribution at all available energies. A sche-

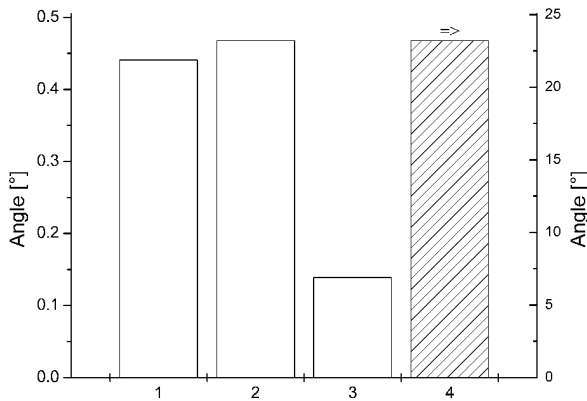


**Fig. 9.** Measured angular divergence of the reflected beam from a copper plate to which different surface treatments were applied. The colour of the bars indicates which scale to use.

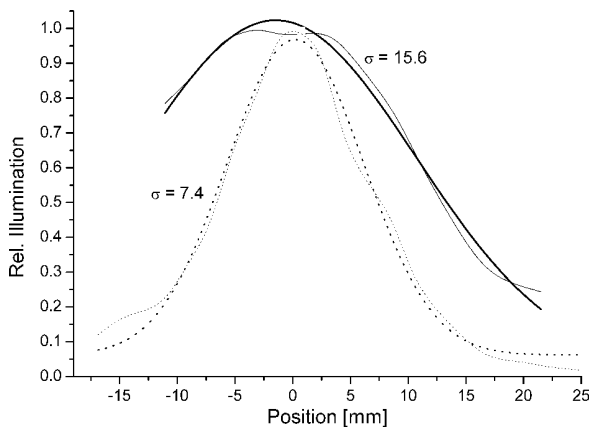


**Fig. 10.** Relative Illumination as a function of beam energy for a diffusive (—) and a non-diffusive (---) OTR screen.

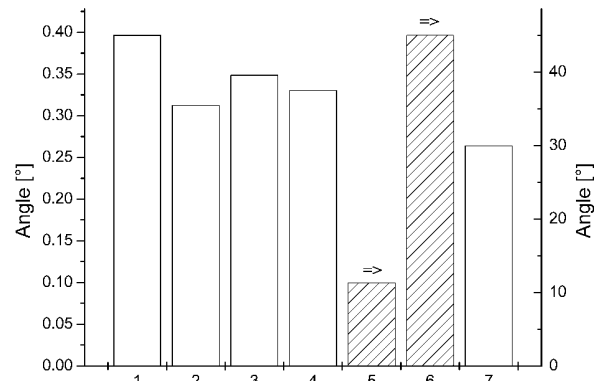


**Fig. 11.** Measured angular divergence of the reflected beam from a stainless steel plate to which different surface treatments were applied. The colour of the bars indicates which scale to use.

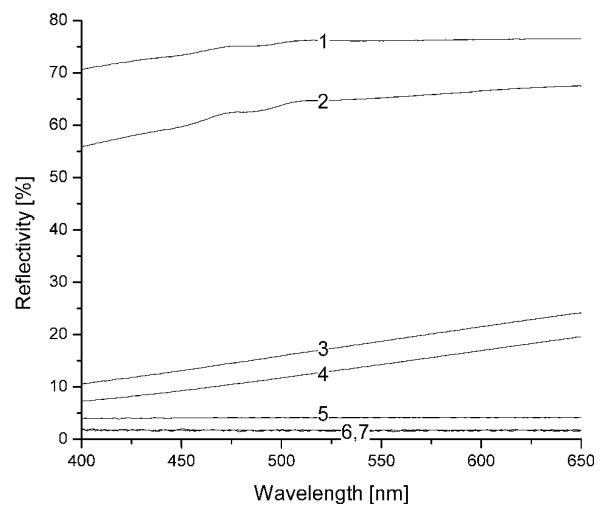


**Fig. 12.** Reflectivity of an aluminium plate after different treatments.

matic drawing of the intended widening of the light distribution is given in the following Fig. 6.

First measurements were done in the past in our optical lab [10], demonstrating the possibility to change this initial opening angle within a wide range. In order to have a base for further investigations, three different screen substrates, namely copper, stainless steel and aluminum were chosen. The test screens consisted of rectangular plates of a size of 100 mm x 50 mm x 5 mm which were first polished to mirror quality and then treated by various mechanic or chemical techniques, ranging from etching to rather aggressive sand blasting. These were applied to several possible screen materials and the resulting light characteristics were determined, see Tables 2 - 4 and Figs. 8 - 13.

These measurements demonstrate that the initial opening angle is very sensitive to these treatments and can be changed in a controlled way between a few tenths of a degree up to completely diffusive behaviour. Surface treatment techniques can thus provide means to re-generate conditions as they are found at lower energies and to avoid the before mentioned problems.

Measurements with beam were then done at CTF3 to confirm this positive effect. For that purpose, a diffusive Aluminium screen that increases the initial opening by approximately  $0.4^\circ$  was installed at the spectrometer screen MTV0605, where electron beam energies between 95 and 115 MeV were available. This data could directly be compared to earlier measurements done at the

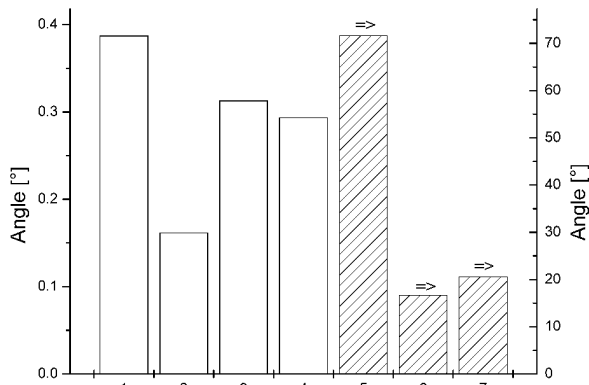


**Fig. 13.** Measured angular divergence of the reflected beam from an aluminium plate to which different surface treatments were applied. The colour of the bars indicates which scale to use.

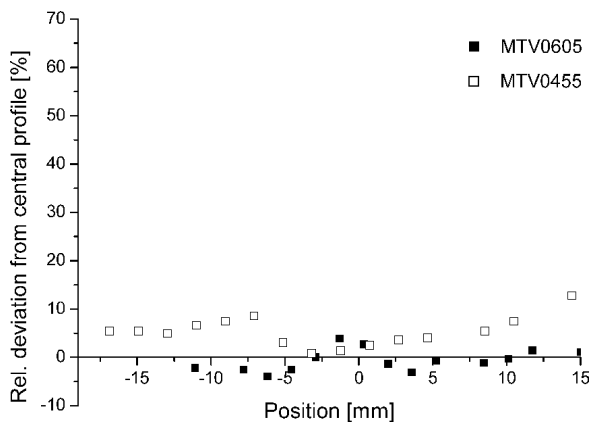


**Fig. 14.** Relative deviation of beam width at different screen positions with respect to average width.

same beam energy at spectrometer system MTV0455.

As can be seen in Fig. 10, the change in illumination with the diffusive screen towards the screen edges was smaller by at least a factor of two as compared to the system with a reflective screen. The light level stayed practically constant over a large part of the central screen region and decreased to values below 50% of the central light level only at the far edge of the screen. Furthermore, the deviation of the beam width, determined at each of the different positions across the screen, could practically be eliminated, Fig. 14. While deviations up to more than 50% in comparison to the central reference profile were observed in earlier measurements, this variation stayed below the 5% level in all measurements with the diffusive screen.

Changing the existing screens against diffusive ones thus is a simple possibility to reduce the nega-

**Table 2.** Overview of treatments applied to copper screens after polishing.

Treatment Number	Description
1	Vibratory finishing, 15 Min.
2	HCl + CrO <sub>3</sub>
3	CrO <sub>3</sub> + H <sub>2</sub> S <sub>2</sub> O <sub>8</sub>
4	HCl + CrO <sub>3</sub> + H <sub>3</sub> PO <sub>4</sub>

**Table 3.** Overview of treatments applied to stainless steel screens after polishing.

Treatment Number	Description
1	Degreasing
2	Degreasing + HNO <sub>3</sub> + HF
3	Degreasing + HNO <sub>3</sub> + HF + NaOH
4	Oxidation
5	Glass bead blasting
6	Sand blasting
7	Vibratory finishing, 15 Min.

**Table 4.** Overview of treatments applied to aluminium screens after polishing.

Treatment Number	Description
1	Diffusive Screen
2	Degreasing
3	Degreasing + HNO <sub>3</sub> + HF
4	Degreasing + HNO <sub>3</sub> + HF + NaOH
5	Silver coating
6	Glas bead blasting
7	Sand blasting

tive effects observed at higher beam energies. A clear advantage is that all screen supports can be kept unaltered and only the mounted foil needs to be changed, guaranteeing a smooth transition and a low-cost solution of this problem.

For some applications however, like e.g. the determination of the beam energy or the beam divergence, it is highly desirable to directly measure the

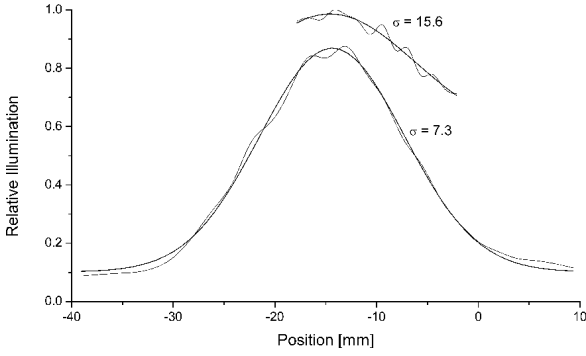


**Fig. 15.** Relative Illumination as a function of beam energy with a flat (—) and a parabolic (---) OTR screen.

opening angle of the OTR light. For these measurements, different techniques need to be applied.

#### 4. PARABOLIC SUPPORT

An alternative approach to limit the vignetting effect caused by the optical system is to use a curved screen instead of a flat one. A parabolic shape  $y = x^2 / (4f)$  along the horizontal axis focuses the light in this plane at a distance  $f$ . It thus can be used to make sure that no emitted light is vignetted by the first lens of the optical system, typically placed at a distance of  $\sim 50$  cm.

The resulting energy distribution by frequency  $\omega$  and observation angle  $\theta$  can then be calculated by [11]

$$W = \frac{\omega^2 q^2}{4\pi^4 c^3} \left| \int dx dy \frac{\omega}{\gamma v} \frac{x}{r} \cos \theta K_1 \left( \frac{\omega r}{\gamma v} \right) e^{-i\vec{k}\vec{r}} \right|^2, \quad (3)$$

where  $\gamma$  is the Lorentz factor and  $v$  the electron velocity. Any arbitrary surface given by  $z(x,y)$  is expressed by the phase factor  $\vec{k} \cdot \vec{r} = k(x \sin \theta + z(x,y) \cos \theta)$ .

The relative illumination of the camera was greatly improved by the parabolic screen, Fig. 15. It stayed uniform over practically the entire usable surface. Due to the fact that the support was probably installed in the vacuum chamber at an unwanted tilt angle and problems related to the mounting of the foil, only a smaller screen area was used in measurements and local position-dependent changes in illumination were found. The focal length of the support was  $f = 500$  mm, which corresponds to the distance to the first lens.

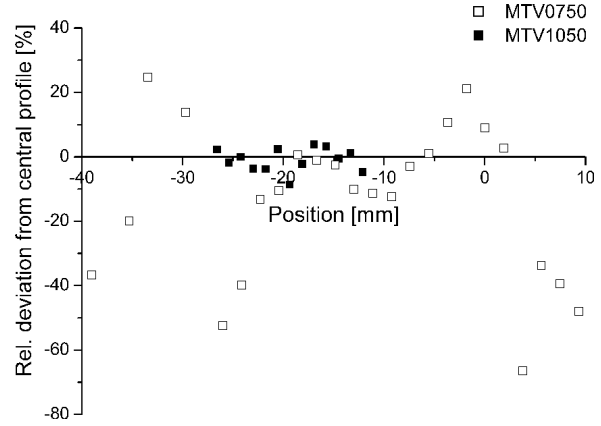


**Fig. 16.** Relative deviation of beam width at different screen positions with respect to average width.

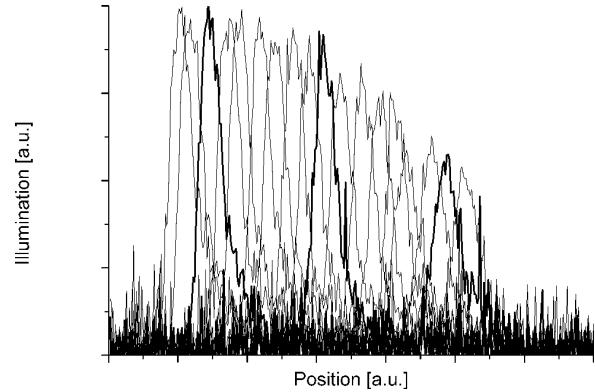


**Fig. 17.** Measured intensity distribution at 100 MeV with a non-diffusive screen.

Already at this relatively low beam energy measured beam widths changed greatly in the past, Fig. 16. With the parabolic screen the measured beam width at different positions across the screen stayed basically identical to the one obtained in measurements at the screen centre.

Due to the initial focusing effect of the parabolic surface, the overall light level is higher than in comparable measurements with a flat screen. In addition, the shape of the distribution is basically maintained throughout the scan and thus provides a reliable measurement even at positions far off-centre, Fig. 17. The improvement in both, the level of light away from the screen centre and the shape of the different distributions, can be clearly seen.

#### 5. CONCLUSION

Different methods to reduce the vignetting effect observed at high beam energies at CTF3 were investigated. Measurements using a diffusive screen

with the aim to increase the initial opening angle of the emitted OTR proved results found in the lab and improved the measurements substantially. The results obtained by using a parabolic support to provide an initial focusing of the emitted light were equally good and will probably become the future standard in CTF3 after the encountered problems with screen and foil mounting are solved.

## REFERENCES

- [1] L. Wartski, S. Roland, J. Lasalle, M. Bolore and G. Filippi // *J. Appl. Phys.* **46** (1975) 3644.
- [2] L. Wartski, *Etude du rayonnement de transition optique produit par des électrons d'énergie 30 à 70 MeV. Application aux diagnostics de faisceaux de particules chargées* (Thesis at the Université de Paris-Sud, 1976).
- [3] D.W. Rule and R.B. Fiorito, In: *AIP Conf. Proc.* (1991) 229.
- [4] X. Artru, R. Chehab, K. Honkavaara and A. Variola // *Nucl. Instr. Meth. B* **145** (1998) 160.
- [5] *CTF3 Design Report*, ed. by G. Geschonke and A. Ghigo ( CERN/PS 2002-008, RF).
- [6] CLIC Study Team, *Proposal for Future CLIC Studies and a New CLIC Test Facility (CTF3)* (CERN/PS 99-047 (LP) and CLIC Note 402, 1999).
- [7] C.P. Welsch, E. Bravin and T. Lefèvre, In: *Proc. Europ. Part. Acc. Conf., Edinburgh, Scotland (2006)* (CERN-AB-2006-069, CLIC note 687, and CTF3 note 082).
- [8] <http://www.esrf.fr/computing/scientific/xop2.1/>
- [9] <http://www.zemax.com>
- [10] C.P. Welsch, H. Braun, E. Bravin, R. Corsini, T. Lefevre, D. Schulte and F. Tecker, In: *Proc. DIPAC, Lyon, France (2005)*, (CERN-AB-2005-066 and CLIC note 660).
- [11] S. Reiche and J.B. Rosenzweig, In: *Proc. Part. Acc. Conf., Chicago, USA (2001)*.